Available online at www.sciencedirect.com
SCIENCE DIRECT®
Journal of Solid State Chemistry 178 (2005) 2218–2224
JOURNAL OF SOLID STATE CHEMISTRY
www.elsevier.com/locate/jssc

Low-temperature and high-pressure structural behaviour of $NaBi(MoO_4)_2$—an X-ray diffraction study

A. Waśkowska[a,*], L. Gerward[b], J. Staun Olsen[c], M. Mączka[a], T. Lis[d], A. Pietraszko[a], W. Morgenroth[e]

[a]*Institute of Low Temperature and Structure Research, Polish Academy of Sciences, P.O.B. 1410, 50 950 Wrocław, Poland*
[b]*Department of Physics, Technical University of Denmark, 2800 Kongens Lyngby, Denmark*
[c]*Niels Bohr Institute Oersted Laboratory, University of Copenhagen, 2100 Copenhagen, Denmark*
[d]*Faculty of Chemistry, University of Wrocław, 14 F. Joliot-Curie, 50 383 Wrocław, Poland*
[e]*Hamburg Synchrotron Radiation Laboratory, Hasylab, at Desy, 22603 Hamburg, Germany*

Received 23 February 2005; received in revised form 29 April 2005; accepted 2 May 2005
Available online 1 June 2005

Abstract

$NaBi(MoO_4)_2$ has been characterized by single-crystal and powder X-ray diffraction in the temperature and pressure ranges 13–297 K and 0–25 GPa, respectively. The domain structure developing below $T_c = 241$ K proves that $NaBi(MoO_4)_2$ undergoes a ferroelastic phase transition associated with tetragonal $I4_1/a$ to monoclinic $I2/a$ symmetry change. The character of the unit cell evolution as a function of temperature indicates a continuous transition with the spontaneous strain as an order parameter. The structural distortion, due to small displacements of Bi^{3+} and Na^+ ions, develops slowly. Therefore the overall changes, as measured in single-crystal diffraction at 110 and 13 K, appear to be subtle. High-pressure powder X-ray diffraction shows that the elastic behaviour is anisotropic, the linear compressibility along the *a*- and *c*-axes of the tetragonal unit cell being $\beta_a = 2.75(10) \times 10^{-3}$ and $\beta_c = 4.30(10) \times 10^{-3}\,GPa^{-1}$, respectively. The cell contraction, stronger along the *c*-axis, causes the distances between the MoO_4 layers to be shortened. Consequently, the cation migration in the channels formed by MoO_4 tetrahedra becomes hindered, and any symmetry lowering phase transition is not observed up to 25 GPa. The zero-pressure bulk modulus is $B_0 = 76(5)$ GPa, and its pressure derivative $B_0' = 5.1(5)$.

Keywords: Molybdates; Phase transition; Low temperature; High pressure; X-ray diffraction

1. Introduction

A series of double molybdates $M^IM^{III}(MoO_4)_2$, (M^I = alkali metal, M^{III} = trivalent element), form a class of materials, which can be used in catalysis and as acousto-optic devices or solid-state laser media. Information on the structural stability in a wide temperature or pressure range is important for many applications of these materials. Some double molybdates with trigonal structure are known to undergo phase transitions of ferroelastic/ferroelectric nature. Typical examples are $KSc(MoO_4)_2$ [1], $K_3Na(MoO_4)_2$ [2], which become monoclinic at low temperature. Scheelite-type tetragonal molybdates have a random distribution of M^I M^{III} ions at the Ca site, and tetrahedrally coordinated Mo at the W site (the prototype Scheelite, $CaWO_4$, has space group $I4_1/a$ [3]). The crystals can be used as a host lattice for optically active rare-earth ions, since M^{III} can be replaced with ions having luminescence properties. $NaLa(MoO_4)_2$ doped with Nd^{3+}, Er^{3+} and Tm^{3+} ions has been suggested for laser materials in crystallographic and optical studies [4]. Recently, $NaBi(MoO_4)_2$ was shown to be a promising laser medium [5–7]. Useful

*Corresponding author. Fax: +48 71 344 1029.
E-mail address: waskowsk@int.pan.wroc.pl (A. Waśkowska).

0022-4596/$ - see front matter © 2005 Elsevier Inc. All rights reserved.
doi:10.1016/j.jssc.2005.05.001

catalytic activity has been observed in nonstoichiometric $Na_{0.5-x}M^{III}_{0.5+x/3}\square_{2x/3}MoO_4$, where $x = 0$ and 0.18 and M^{III} = Bi, Ce or La, where the M^{III} site is partially vacant and there is no long-range ordering of the vacancies [8,9].

Earlier studies on the basis of powder neutron and X-ray diffraction data for $NaBi(MoO_4)_2$ [10] and $NaBi(WO4)_2$ [10,11] reported either Scheelite-like structure with space group $I4_1/a$ or slightly distorted Scheelite structure with space group $I\bar{4}$ [12,13]. From our most recent examination of $NaBi(WO_4)_2$, however, it is clear that the exact crystal symmetry is $I4_1/a$ [14] and the previously observed symmetry lowering possibly is due to non-stoichiometry. Small anomaly arriving at about 241 K in the dielectric permittivity measured as a function of temperature was interpreted as a structural phase transition [15]. The transition, however, has not been confirmed with other experimental methods.

In the present work, the effect of low temperature or high pressure on the structural stability of stoichiometric $NaBi(MoO_4)_2$ has been investigated using single-crystal and powder X-ray diffraction. It was expected that the random distribution of Na and Bi ions in 4*b* Wyckoff position at ambient conditions should be replaced by a long-range ordering at low temperature or high pressure, entailing further structure modification. It was foreseen that small displacements of the ions from the positions of the Scheelite-type structure should be difficult to observe. Therefore, the low-temperature measurements of the unit-cell dimensions were performed using X-ray single-crystal diffraction, taking advantage of the inherent high intensity and good collimation of synchrotron radiation. Structure determinations at 110 and 13 K were performed using a conventional X-ray source, the results being compared with the room-temperature data. High-pressure effects were investigated using energy-dispersive powder X-ray diffraction (EDXPD) and synchrotron radiation.

2. Experimental

Single crystals of $NaBi(MoO_4)_2$ were grown by the Stober method based on congruent melting at 1100 K of a stoichiometric mixture of chemically pure Na_2CO_3, Bi_2O_3 and MoO_3. The resulting crystals were colourless and of optical quality.

The temperature dependence of the unit-cell parameters was measured with a Huber 4-circle diffractometer at station D3 of the Hamburg Synchrotron Radiation Laboratory (Hasylab). The wavelength was $\lambda = 0.7000$ (Å). Sample (**I**) was cooled in the range 100–300 K by an Oxford Cryosystem attachment based on liquid nitrogen. At each temperature, the lattice dimensions were calculated by a least-squares refinement using the setting angles of 32 Bragg high-angle reflections in the range $72.0^\circ \leqslant 2\theta \leqslant 74.2^\circ$.

Intensity data were obtained with a single-crystal diffractometer equipped with a CCD detector (KM-4/CCD, Oxford Diffraction), operating in κ geometry and using graphite monochromated Mo$K\alpha$ radiation. For the intensity data collection at 110 and 13 K, sample (**II**) of the same batch was cooled with an Oxford Cryosystem (liquid nitrogen) and an Oxford Helijet (liquid helium), respectively. The intensities were measured in ω-scan geometry, in steps of $\Delta\omega = 1.2^\circ$, the exposure being 20 s per frame. At 110 K, eight sets of 153 exposures at different ω positions covered about 96% of the Ewald sphere. Crystal and instrument stability was controlled by one image, selected as a standard and measured after each 50 images. Because of angular limitations imposed by the Helijet, there were only five sets of exposures at 13 K, which affected the redundancy of the data but had no influence on the resolution. The intensities, corrected for Lorentz-polarization effects, were integrated by means of the CrysAlis program [16]. Absorption was corrected using the symmetry equivalent reflections and optimizing the shape of the crystal measured with a high-resolution telescope [17]. Crystal data and experimental details are summarized in Table 1 together with the parameters of the structure refinements. The electron density residuals of 2.84 and $-2.01\,e\text{Å}^{-3}$ for sample (**I**) were located at the distances 0.28 and 0.29 Å from the 4*b* site. The reason for this remnant electron density can partly be an artefact of not adequately compensated absorption correction and also of some anharmonicity in the atomic thermal displacements at room temperature.

High-pressure powder X-ray diffraction measurements were performed at room temperature using synchrotron radiation and the white-beam energy-dispersive method at station F3 of Hasylab. The diffractometer, working in the energy-dispersive mode, has been described elsewhere [18]. High pressures in the range 0–25 GPa were obtained in a Syassen-Holzapfel-type diamond-anvil cell. The sample and a small ruby chip were placed in a hole of 0.2 mm diameter in a preindented Inconel gasket. A 16:3:1 mixture of methanol, ethanol and water was used as the pressure-transmitting medium. The pressure was determined by the wavelength shift of the ruby R_1 luminescence line, using the non-linear pressure scale of Mao et al. [19]. The Bragg angle was calculated from a zero-pressure diffraction spectrum of NaCl in the diamond anvil cell. The estimated standard deviation (e.s.d.) of the pressure determination is about 0.1 GPa for pressures up to about 10 GPa. For higher pressures, the e.s.d.'s might be larger because of possible non-hydrostatic conditions.

Table 1
Crystal data, experimental details and structure refinement results for $NaBi(MoO_4)_2$

Crystal data	Sample (**I**)	Sample (**II**)	
Temperature (K)	297	110 K	13 K
Crystal system, space group	Tetragonal, $I4_1/a$	Monoclinic, $I2/a$	
Unit cell dimensions (Å)			
a	5.2744(7)	5.263(1)	5.257(1)
b	5.2743(7)	11.553(2)	11.552(2)
c	11.578(2)	5.247(1)	5.233(1)
β		90.18(3)	90.29(3)
Volume (Å^3)	322.09(9)	319.04(11)	317.75(11)
Z, Calculated density (Mg/m^3)	2, 5.690	2, 5.745	2, 5.768
Crystal size (mm)	$0.18 \times 0.17 \times 0.15$	$0.16 \times 0.16 \times 0.14$	
Data collection			
Wavelength (Å)	0.71073	0.71073	
2θ max for data collection	94.50	94.01	118.6
Limiting indices			
h	−10, 10	−10, 10	−3, 12
k	−7, 10	−23, 23	−24, 22
l	−23, 22	−10, 7	−10, 3
Reflections collected	3061	2942	2492
Reflections unique	704	1318	1225
Reflections $>2\sigma(I)$	306	476	664
Absorption coefficient (mm^{-1})	31.16	31.45	31.58
Absorption correction	Analytical	Analytical	
T_{min}, T_{max}	0.667, 0.875	0.783, 0.962	0.810, 0.975
R(int) before, after abs. correction	0.126, 0.062	0.108, 0.047	0.099, 0.030
Refinement			
Refinement method	Full-matrix least-squares on F^2		
Number of refined parameters	14	29	29
Goodness-of-fit on F^2	1.075	0.991	1.045
Final R indices $[I>2\sigma(I)]$			
R_1	0.034	0.021	0.023
wR_2	0.072	0.051	0.034
Largest diff. peak and hole (eÅ^{-3})	2.84 and −2.01	1.12 and −0.93	0.9 and −0.85

3. Results

3.1. Low-temperature studies

The evolution of the tetragonal unit-cell dimensions with temperature at ambient pressure is shown in Fig. 1. At room temperature, the a- and b-axes as well as the unit-cell angles are perfectly consistent with tetragonal symmetry. However, beginning from about 240 K upon cooling, the two axes start to diverge from each other. Although the difference is initially less than the standard deviations, the tendency holds down to 13 K, the lowest temperature of the present study. Near T_c, a permutation between the a- and b-axes is observed. The difference between the two cell dimensions, increasing gradually with decreasing temperature, and the increase of the γ angle, together with accompanying interim α and β fluctuations, reflect a systematic departure from tetragonal symmetry; the low-temperature phase becomes monoclinic. In terms of the Landau theory, such phenomena are associated with a continuous phase transition.

Fig. 1 clearly shows that the structural effect of the transition is not very pronounced in the vicinity of $T_c = 240$ K. However, it was expected to be more marked at lower temperatures. Therefore X-ray intensity data for structure determination were collected at 110 and 13 K.

The room-temperature structure is isomorphic with Scheelite and has unit-cell dimensions $a = 5.2744(5)$ Å, $c = 11.578(2)$ Å. The intensity statistics and systematic absences (hkl: $h+k+l = 2n+1$ and $hk0$: $h,(k) = 2n+1$, $00l$: $l = 4n+1$) uniquely point to the space group $I4_1/a$ (No. 88). The Na and Bi ions sharing the same 4b site were refined with site occupancy factors (SOF) that were allowed to vary. The deviation from

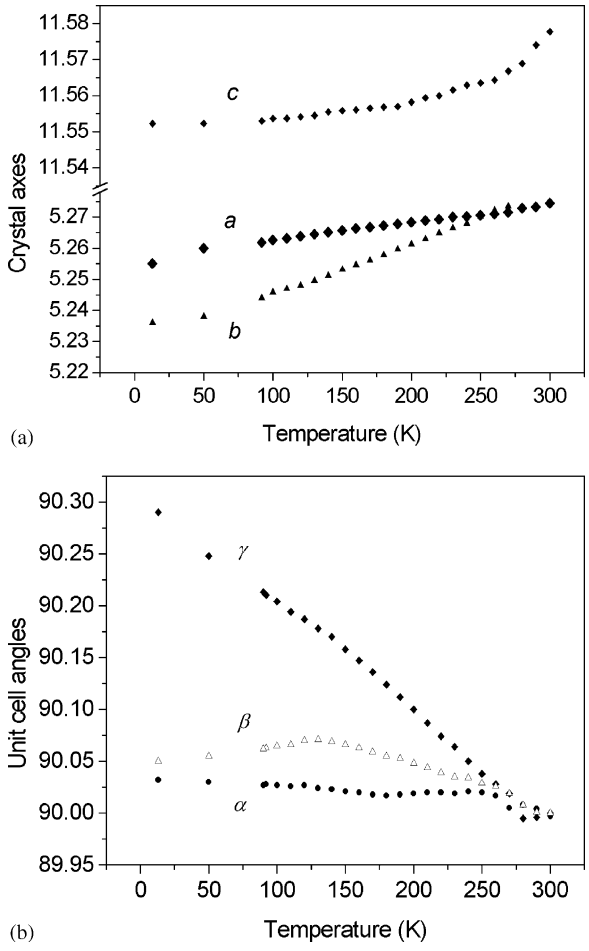

Fig. 1. Temperature-dependent evolution of the tetragonal unit-cell parameters of $NaBi(MoO_4)_2$. (a) Unit-cell axes, (b) unit-cell angles.

Table 2
Atomic positions and equivalent isotropic displacement parameters ($Å^2 \times 10^4$) for NaBi $(MoO_4)_2$ at room temperature

Ion	Position	x/a	y/b	z/c	U_{iso}, U_{eq}
Bi/Na	4*b*	0.0	0.25	0.625	173(2)
Mo	4*a*	0.0	0.25	0.125	106(1)
O	16*f*	0.1494(5)	0.4888(5)	0.2084(3)	250(2)

Note: The positions correspond to the second setting of space group $I4_1/a$ (# 88) in the International Tables for Crystallography [39].

stoichiometry was found to be less than 1%, and therefore the site occupancy 0.5 was assumed. The atomic positions are given in Table 2.

Overall intensity statistics for the 110 K data indicated the pseudotetragonality. However, the intensities of the Bragg reflections, such as, e.g. 0 0 2, 0 0 6 and 3 3 0 (absent in $I4_1/a$, but permitted below T_c), which in terms of the Landau theory could have been a measure of the square of the order parameter, were still within the experimental error. A trial structure refinement with symmetry $I4_1/a$ converged well. Nevertheless, somewhat high amplitudes of the equivalent isotropic displacements for Bi^{3+} and Na^+ compared with the thermal parameters of Mo and O-atoms, could reflect positional fluctuations or static deviations from tetragonal symmetry. Also, a splitting in ω-scan profiles occurring below T_c for numerous strong reflections, was a sign of the presence of a lower symmetry domain structure in the crystal, and thus of ferroelastic properties.

The space group extinctions for the 13 K data $\{h\,k\,l$: $h+k+l=2n+1$ and $h\,0\,l$: $h,(l)=2n+1\}$ were consistent with space group $I2/a$ (No. 15). The standard setting, $C2/a$ can be obtained with the transformation matrix $(-1\,1\,0;\ 1\,1\,0;\ \frac{1}{2},-\frac{1}{2},-\frac{1}{2})$, leading to a cell of dimensions $a=7.413$, $b=7.748$, $c=6.842$ Å, $\beta=122.55°$, $V=318.5$ Å^3. However, this cell does not show any apparent relationship to the Scheelite-like phase. Therefore, after the cell transformation $a_t=c_m$, $b_t=a_m$, and $c_t=b_m$ (where the indices t and m refer to tetragonal and monoclinic cell, respectively), the structure was solved in $I2/a$ using the SHELXS97 program [20]. As the thermal displacements of Bi^{3+} and Na^+ are strongly correlated, they were refined isotropically in separate cycles of calculations. The other atoms were refined with anisotropic thermal displacement parameters. Structure refinements were performed using the SHELXL99 package [21].

Final atomic parameters for the structure at 13 K are given in Table 3. Also shown are the parameters for the structure at 110 K (in italics), re-determined in the space group $I2/a$. A view of the monoclinic structure is shown in Fig. 2. The MoO_4 tetrahedra form the chains around the eight-fold coordinate Bi^{3+} and Na^+ ions. The two ions are displaced along the monoclinic axis in opposite direction with respect to their high-symmetry location at $y=0.625$. Selected interatomic distances are given in Table 4.

Table 3
Atomic positions and equivalent isotropic displacement parameters ($Å^2 \times 10^4$) for NaBi $(MoO_4)_2$ at 13 and 110 K (in italics)

Ion	Position	x/a	y/b	z/c	U_{eq}
Bi	4(*e*)	0.25	0.62335(4)	0.0	92(1)
		0.25	*0.62281(7)*	*0.0*	*92(2)*
Na	4(*e*)	0.25	0.6436(4)	0.0	81(6)
		0.25	*0.6378(17)*	*0.0*	*110(10)*
Mo	4(*e*)	0.25	0.12475(4)	0.0	59(1)
		0.25	*0.12495(7)*	*0.0*	*56(1)*
O1	8(*f*)	0.1032(4)	0.0420(2)	0.2383(5)	121(3)
		0.1016(7)	*0.0394(3)*	*0.2391(5)*	*93(4)*
O2	8(*f*)	0.0092(4)	0.2090(2)	−0.1475(7)	100(3)
		0.0083(6)	*0.2075(3)*	*−0.1516(6)*	*137(5)*

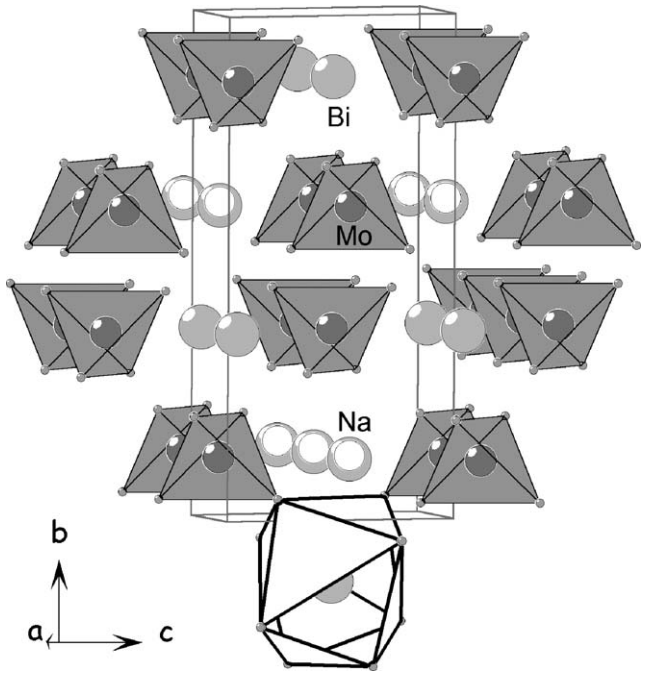

Fig. 2. Crystal structure of $NaBi(MoO_4)_2$ in the monoclinic phase. For clarity, the coordination polyhedron around only one Bi^{3+} cation is shown (bold outlined).

Table 4
Selected interatomic distances (in Å) for $NaBi(MoO_4)_2$ at given temperatures

Ions		297 K	110 K	13 K
Bi	–O1	2.497(3) 4 ×	2.447(3) 2 ×	2.454(2)
	–O2		2.476(3) 2 ×	2.481(2)
	–O1	2.500(3) 4 ×	2.498(3) 2 ×	2.488(2)
	–O2		2.516(5) 2 ×	2.483(2)
	–O1			2.489(2)
	–O2			2.502(2)
	–O1			2.505(2)
	–O2			2.505(2)
Na	–O1	2.497(3) 4 ×	2.570(3) 2 ×	2.583(2)
	–O2		2.384(3) 2 ×	2.306(2)
	–O1	2.500(3) 4 ×	2.583(8) 2 ×	2.604(2)
	–O2		2.413(3) 2 ×	2.325(2)
	–O1			2.638(2)
	–O2			2.400(2)
	–O1			2.675(2)
	–O2			2.419(2)
Mo	–O1	1.772(3) 4 ×	1.776(3) 2 ×	1.742(2)
	–O2		1.780(3) 2 ×	1.763(2)
	–O1			1.764(2)
	–O1			1.778(2)

The bond angles in MoO_4 tetrahedra vary from 107.3(1)–114.6(1)° and the O–Bi/Na–O angles are in the range 68.3(1)–152.9(2)°.

Further details of the crystal structure investigations can be obtained from the Fachinformationszentrum Karlsruhe, 76344 Eggenstein-Leopoldshafen, Germany, (fax: 49 7247 808 666; e-mail: crysdata@fiz-karlsruhe.de) on the depository numbers; 415131, 415132 and 415133 for the data at 293, 110 and 13 K, respectively.

3.2. High-pressure studies

Within the resolution of the EDXRD method, the high-pressure diffraction spectra can be indexed according to the tetragonal unit cell in the whole pressure range. The unit-cell dimensions, a and c, as functions of pressure are shown in Fig. 3. The pressure has been limited to the range 0–14 GPa to avoid any possible influence of non-hydrostatic conditions. The corresponding linear compressibilities, β_a and β_c, are given by

$$\beta_a = 2.75(10) \times 10^{-3}\,\mathrm{GPa}^{-1}, \text{ and}$$
$$\beta_c = 4.30(10) \times 10^{-3}\,\mathrm{GPa}^{-1}. \quad (1)$$

The unit-cell volume as a function of pressure can be described by the Birch–Murnaghan equation of state [22]:

$$P = \tfrac{3}{2}B_0(x^{-7/3} - x^{-5/3})\left[1 - \tfrac{3}{4}(4 - B_0')(x^{-2/3} - 1)\right], \quad (2)$$

where $x = V/V_0$, V being the volume at pressure P, and V_0 the volume at zero pressure, B_0 is the bulk modulus and B_0' its pressure derivative, both parameters evaluated at zero pressure. The relative volume, V/V_0, as a function of pressure is shown by the inset of Fig. 3. A least-squares fit of the Birch–Murnaghan equation (2) to the experimental pressure–volume points gives

$$B_0 = 76(5)\,\mathrm{GPa}, \text{ and } B_0' = 5.1(5). \quad (3)$$

The bulk modulus can also be obtained from the elastic constants using ultrasonic data and the

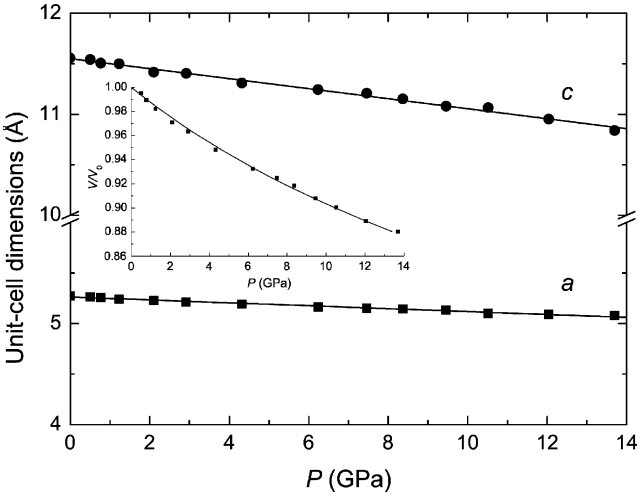

Fig. 3. Unit-cell dimensions, a and c, of tetragonal $NaBi(MoO_4)_2$ as functions of pressure. The inset shows the pressure dependence of the relative volume, V/V_0.

Table 5
Bulk moduli of some Scheelite-type molybdates

Compound	B_0	B_0'	Method	Reference
$NaBi(MoO_4)_2$	75(5)	5.1(5)	XRD	Present work
$SrMoO_4$	73		Ultrasonics	[24]
$PbMoO_4$	73.1		Ultrasonics	[25]
$PbMoO_4$	73		Ultrasonics	[24]
$PbMoO_4$	64(2)		XRD	[26]
$CaMoO_4$	80		Ultrasonics	[24]
$CaMoO_4$	81.5(7)		XRD	[26]
$CaWO_4$	68(9)		XRD	[26]
$CaWO_4$	77(8)	4.9(9)	XRD	[27]

For comparison, data for the prototype Scheelite $CaWO_4$ are also given. XRD = X-ray diffraction.

expression [23]

$$B_0 = \tfrac{1}{9}(2c_{11} + c_{33} + 2c_{12} + 4c_{13}), \quad (4)$$

where c_{ij} are the elastic stiffness constants.

Although there is some scatter in the published data, our value for the bulk modulus of $NaBi(MoO_4)_2$ is in good agreement with those previously determined by ultrasonic techniques and X-ray diffraction as seen in Table 5. Farley et al. [24] have pointed out that among the molybdates, the resistance to both tensile and shear deformation decreases with increasing molar mass. The molar mass of $(NaBi)_{0.5}MoO_4$ is in between those of $SrMoO_4$ and $PbMoO_4$, and accordingly, our value for the bulk modulus is in good agreement with those for $SrMoO_4$ and $PbMoO_4$ [24,25]. It is also worth noting that the values of B_0 and B_0' resulting from the present study on $NaBi(MoO_4)_2$ are similar to those found for the prototype Scheelite $CaWO_4$ [26,27].

4. Discussion

As in other Scheelite-related compounds, e.g. $BiVO_4$ [28–30], $LaNbO_4$ [31], $YNbO_4$ [32,33] and $CaMoO_4$ [34], the tetragonal-to-monoclinic transition does not show up very clearly. Based on diffraction data from a wide temperature range we attempt to propose a model of the structural mechanism driving the transition.

At room temperature, due to symmetry constraints, the Mo–O distances of the MoO_4 tetrahedra must be equal. The Bi^{3+} and Na^+ ions, at their eight-fold coordination sites, form four shorter and four longer Me–O distances (Table 4). On cooling, a systematic cell-contraction causes an accumulation of strain at the 4*b* site of the tetragonal cell, randomly occupied by the two species differing in atomic number ($Z_{Bi} = 83$, $Z_{Na} = 11$), and consequently differing in electronic structure and scattering power. The continuous strain results in a displacement of the two ions, thus lowering the symmetry of the site and hence inducing a change in intensities of certain reflections. At 110 K the intensities of the symmetry-breaking reflections are only marginal and the overall intensity statistics is inconclusive. Nevertheless, the coordination polyhedron about Bi^{3+} and Na^+ becomes distorted, compared with the tetragonal structure. There are now four pairs of somewhat different Bi–O and Na–O distances (Table 4).

For the 13 K data the structure calculations show the Bi^{3+} ions in 4*e* displaced from their high-symmetry position by −0.019(1) Å along the *b*-axis, while the Na^+ ions are shifted in the opposite direction by 0.215(5) Å. Consequently, the metal ion surroundings become further distorted, including also the MoO_4 tetrahedron. At this temperature all eight Me–O distances are different, ranging from 2.454(2) to 2.505(2) Å for Bi^{3+}, and from 2.306(2) to 2.675(2) Å for Na^+. It is remarkable that the Mo^{6+} ion retains its high-symmetry location in the whole temperature range, although it could move along the *b*-axis in accordance with its 4(*e*) position. Therefore, the deformation of the MoO_4 tetrahedron results mainly from the oxygen displacements.

The former studies on simple Scheelite-type molybdates and tungstates showed that the decrease of the c/a ratio causes significant increase in metal–metal repulsion, and finally in high-pressure phase transitions into wolframite- or $HgWO_4$-type structures with octahedral coordination of cations [35]. It has been shown that in simple Scheelites, ABX_4, the critical pressure, P_c, was correlated with the BX_4/A radii ratio; the larger this ratio, the higher the pressure P_c [35]. Since Na^+ and Bi^{3+} ions have ionic radii similar to Cd^{2+} and Pb^{2+}, respectively, a high-pressure phase transition should be expected somewhere between 6.5 and 12 GPa, the pressures, which are the P_c values for $PbMoO_4$ [36] and $CdMoO_4$ [37], respectively. In contrast, the present results show that $NaBi(MoO_4)_2$ does not exhibit any transition up to 25 GPa, similarly as $NaLa(MoO_4)_2$ which was stable up to 27 GPa [38].

5. Conclusions

We conclude from the low-temperature measurements that $NaBi(MoO_4)_2$ undergoes a ferroelastic phase transition at about 240 K from space group $I4_1/a$ to $I2/a$ due to small displacements of the Na^+ and Bi^{3+} cations from their high-symmetry position. This structure instability brings about changes in the oxygen positions, and consequently the coordination polyhedra distortion. The evolution in the crystal dimensions is very subtle, and it develops gradually upon cooling. The point group transforms from $4/m$ to $2/m$, which are both centrosymmetric and thus paraelastic. This phase transition of a second order is analogous to those

observed in the isostructural Scheelite-type compounds $BiVO_4$, $LaNbO_4$ and $CaMoO_4$.

The anisotropic nature of the elastic properties of the tetragonal unit cell is illustrated by a difference between the linear compressibility along the *a*- and *c*-axes at high pressure. The unit cell contraction, being stronger along the *c*-axis, results in shortening the distances between the layers of MoO_4 tetrahedra (Fig. 2). In this way the migration of Bi^{3+} and Na^{+} ions within the cavities formed by the MoO_4 layers is prevented. Such a structure distortion would explain an absence of the pressure-induced phase transition. The value of the bulk modulus shows that $NaBi(MoO_4)_2$ is a relatively soft material. An amorphous compound develops at pressures above 20 GPa.

Acknowledgments

We thank HASYLAB-DESY for permission to use the synchrotron radiation facility. Part of this work was supported by the European Community – Research Infrastructure Action under the FP6 *Structuring the European Research Area* Programme (through the Integrated Infrastructure Initiative *Integrating Activity on Synchrotron and Free-Electron Laser Science*). L.G., J.S.O. and A.W. acknowledge financial support from the Danish Natural Science Research Council through DANSYNC.

References

[1] N.A. Kislov, V.V. Mitkevich, J.M. Nesterenko, C.M. Tretyak, Kristallografiya 36 (1991) 1296.
[2] J. Fabry, V. Petříček, P. Vaněk, T. Cisarová, Acta Crystallogr. B 53 (1997) 593.
[3] R.D. Burbank, Acta Crystallogr. 18 (1965) 88.
[4] S.B. Stevens, C.A. Morrison, T.H. Allik, A.L. Rheingold, B.S. Haggerty, Phys. Rev. B 43 (1991) 7386.
[5] M. Rico, V. Volkov, C. Zaldo, J. Alloy Compd. 323 (2001) 806.
[6] M. Rico, V. Volkov, C. Cascales, C. Zaldo, Chem. Phys. 279 (2002) 73.
[7] A. Mendez-Blas, M. Rico, V. Volkov, C. Cascales, C. Zaldo, C. Coya, A. Kling, L.C. Alves, J. Phys.: Condens. Matter 16 (2004) 2139.
[8] R.G. Teller, J. Am. Chem. Soc. 93 (1971) 2622.
[9] A.W. Sleight, K. Aykan, D.B. Rogers, J. Solid State Chem. 13 (1975) 231.
[10] R.G. Teller, Acta Crystallogr. C 48 (1992) 2101.
[11] V. Klevtsov, V.A. Vinokurov, R.F. Klevtsova, Kristallografiya 18 (1973) 1192.
[12] J. Hanuza, A. Benzar, A. Haznar, M. Maczka, A. Pietraszko, J.H. Van der Maas, Vib. Spectrosc. 12 (1996) 25.
[13] J. Hanuza, A. Haznar, M. Maczka, A. Pietraszko, A. Lemiec, J.H. Van der Maas, E.T.G. Lutz, J. Raman Spectrosc. 28 (1997) 953.
[14] M. Maczka, E.P. Kokanyan, J. Hanuza, J. Raman Spectrosc. 36 (2005) 33.
[15] L.N. Pelikh, A.A. Gurskas, Fiz. Tverd. Tela 21 (1979) 218.
[16] CrysAlis CCD, Oxford Difraction Ltd., Wrocław, Poland, 2001.
[17] CrysAlis RED'2004 Release 1.170.14, Oxford Difraction Ltd., Oxford, UK.
[18] J.S. Olsen, Rev. Sci. Instrum. 83 (1992) 1058.
[19] H.K. Mao, J. Xu, P.M. Bell, J. Geophys. Res. 91 (1986) 4673.
[20] G.M. Sheldrick, SHELXS97, Program for Solution of the Crystal Structures, University of Goettingen, 1997.
[21] G.M. Sheldrick, SHELXL99, Program for Crystal Structure Refinement, University of Goettingen, 1999.
[22] F.J. Birch, J. Appl. Phys. 9 (1938) 279;
F.J. Birch, Phys. Rev. 71 (1947) 809.
[23] J.P. Watt, J. Appl. Phys. 50 (1979) 6290.
[24] J.M. Farley, G.A. Saunders, D.Y. Chung, J. Phys. C.: Solid State Phys. 8 (1975) 780.
[25] G.A. Coquin, D.A. Pinnow, A.W. Warner, J. Appl. Phys. 42 (1971) 2162.
[26] R.M. Hazen, W.L. Finger, J.W.E. Mariathasan, J. Phys. Chem. Solids 46 (1985) 253.
[27] D. Errandonea, M. Somayazulu, D. Häusermann, Phys. Stat. Sol. (b) 235 (2003) 162.
[28] A.W. Sleight, H.-Y. Chen, A. Ferretti, Mater. Res. Bull. 14 (1979) 1571.
[29] J.D. Bierlein, A.W. Sleight, J. Geophys. Res. 91 (1986) 4673.
[30] W.I.F. David, I.G. Wood, A.M. Glazer, J. Phys. C 16 (1983) 5127.
[31] L.H. Brixner, J.F. Whitney, F.C. Zumsteg, G.A. Jones, Mater. Res. Bull. 12 (1977) 17.
[32] A.I. Khomkov, Kristallografiya 4 (1959) 836.
[33] G.J. McCarthy, Acta Crystallogr. B 27 (1971) 2285.
[34] J. Simon, J. Banys, J. Hoentsch, G. Völkel, R. Böttcher, A. Hofstaetter, A. Scharmann, J. Phys.: Condens. Matter 8 (1996) L359.
[35] D. Errandonea, F.J. Manjon, M. Somayazulu, D. Häusermann, J. Solid State Chem. 177 (2004) 1087.
[36] A. Jayaraman, B. Batlogg, L.G. Van Uitert, Phys. Rev. B 31 (1985) 5423.
[37] S.R. Shieh, L.C. Ming, A. Jayaraman, J. Phys. Chem. Sol. 57 (1996) 205.
[38] A. Jayaraman, S.Y. Wang, S.K. Sharma, Solid State Commun. 93 (1995) 885.
[39] T. Hahn (Ed.), International Tables for Crystallography, vol. A. Kluwer Academic Publishers, Dordrecht/Boston/London, 1996, pp. 351, 185.